OXFORD

Cerebral Cortex, 2015, 1–11

doi: 10.1093/cercor/bhv018
Original Article

ORIGINAL ARTICLE

NMDA Receptor Antagonist Ketamine Distorts Object Recognition by Reducing Feedback to Early Visual Cortex

Anouk M. van Loon[1,2,3], Johannes J. Fahrenfort[3], Bauke van der Velde[1], Philipp B. Lirk[4], Nienke C. C. Vulink[5], Markus W. Hollmann[4], H. Steven Scholte[1,2,†], and Victor A. F. Lamme[1,2,†]

[1]Department of Brain and Cognition, University of Amsterdam, Amsterdam 1018 XA, The Netherlands, [2]Amsterdam Brain and Cognition, University of Amsterdam, Amsterdam 1018 WS, The Netherlands, [3]Department of Cognitive Psychology, VU University, Amsterdam 1081 BT, The Netherlands, [4]Department of Anesthesiology, Academic Medical Center, University of Amsterdam, Amsterdam 1105 DD, The Netherlands, and [5]Department of Psychiatry, Academic Medical Center, University of Amsterdam, Amsterdam 1105 AZ, The Netherlands

Address correspondence to Anouk M. van Loon, Department of Cognitive Psychology, VU University, Van der Boechorststraat 1, 1081 BT, Amsterdam, The Netherlands. Email: anouk.vanloon@gmail.com

[†]Steven Scholte and Victor A. F. Lamme shared senior authorship.

Abstract

It is a well-established fact that top-down processes influence neural representations in lower-level visual areas. Electrophysiological recordings in monkeys as well as theoretical models suggest that these top-down processes depend on NMDA receptor functioning. However, this underlying neural mechanism has not been tested in humans. We used fMRI multivoxel pattern analysis to compare the neural representations of ambiguous Mooney images before and after they were recognized with their unambiguous grayscale version. Additionally, we administered ketamine, an NMDA receptor antagonist, to interfere with this process. Our results demonstrate that after recognition, the pattern of brain activation elicited by a Mooney image is more similar to that of its easily recognizable grayscale version than to the pattern evoked by the identical Mooney image before recognition. Moreover, recognition of Mooney images decreased mean response; however, neural representations of separate images became more dissimilar. So from the neural perspective, unrecognizable Mooney images all "look the same", whereas recognized Mooneys look different. We observed these effects in posterior fusiform part of lateral occipital cortex and in early visual cortex. Ketamine distorted these effects of recognition, but in early visual cortex only. This suggests that top-down processes from higher- to lower-level visual areas might operate via an NMDA pathway.

Key words: fMRI, Mooney, MVPA, object, perception, top-down

Introduction

Our visual system is well equipped to transform sensory input into distinguishable object representations. For a long time, it this was thought that this was a strictly hierarchical operation, where representations become increasingly complex going up the hierarchy, as receptive field size increases (Hubel and Wiesel 1968). However, recently it was shown that object recognition

alters object representations also in early visual cortex (Hsieh et al. 2010) and even that the contents of visual working memory and mental imagery can be successfully decoded from the activity patterns in early visual areas (Harrison and Tong 2009; Albers et al. 2013; Vetter et al. 2014). These studies are in line with the idea that activity in early visual areas not simply reflects the sensory input but are influenced by top-down information (Rao and Ballard 1999; Hochstein and Ahissar 2002; Lee and Mumford 2003; Friston 2005; Bar et al. 2006; Lamme 2006; Yuille and Kersten 2006; Summerfield and Koechlin 2008). But what could be the underlying neural mechanism of this top-down processing?

It is suggested by modeling studies that top-down activity operates via feedback connections that largely depend on the N-methyl-D-aspartate (NMDA)-pathway (Lumer et al. 1997; Dehaene et al. 2003). Opening of the NMDA receptors is gated by postsynaptic depolarization, and therefore, the effect of feedback will be most pronounced if the neurons are first depolarized by sensory input (Ekstrom et al. 2003). Physiological evidence supports such gating of feedback by feedforward activation (Roelfsema et al. 2002). Moreover, when an NMDA antagonist was injected in the primary visual cortex of macaque monkeys, feedback activity was reduced, whereas feedforward activity was relatively unaffected (Self et al. 2012). However, no attempts have been made to investigate the effects of NMDA receptor manipulation on top-down processes in humans. Therefore, we combined a subanesthetic dose of ketamine, a noncompetitive NMDA antagonist (Lodge and Johnson 1990), with fMRI multivoxel pattern analysis of object representations in the visual cortex. Ketamine—at the dosage used here—primarily targets the NMDA receptor and is often used to study the role of NMDA receptors in human cognition (see, for a review, Newcomer and Krystal (2001)). We used Mooney images (Mooney 1957; Moore and Cavanagh 1998), because recognition of Mooney images typically requires prior knowledge about the image, which we hypothesize to be mediated by top-down processing. We first looked at the neural representation of Mooney images to identification, then provided top-down prior knowledge by showing the grayscale version of that Mooney image, and then looked at the neural representation of the Mooney images again, which were now much easier to recognize. We compared the neural representations of the Mooney and grayscale images in the posterior fusiform part of lateral occipital complex (pFs), an area associated with high-level processing of visual objects, and visual areas V1, V2, V3, and V4. We expected to observe effects of recognition both in pFs and visual areas. We hypothesized that ketamine would mainly interfere with the top-down influence of prior knowledge and, hence, interfere with the recognition effects in early visual areas, but not in pFs.

Materials and Methods

Participants

Twenty healthy subjects (11 males, M = 23.25 years of age, SD = 1.07 years) participated in the study. All subjects were screened for psychiatric disorders, drug addiction, and physical condition. Subjects had normal or corrected-to-normal vision. Subjects were required to refrain from recreational drug usage for 30 days prior to participation and to have had no prior experience with ketamine. All provided written informed consent. The experiment was approved by the Medical Ethical Committee of the University of Amsterdam. Five subjects were excluded due to low vigilance (2 subjects) during scanning, 2 due to excessive movement (>1 mm), and 1 subject due to technical failure. All analyses are based on the remaining 15 subjects (7 males and 8 females, M = 23.24 years of age, SD = 1.20 years).

Stimuli

For each session, we used a set of 12 natural scene photo images (24 in total for the 2 sessions: ketamine vs. placebo). Each set was divided into 2 main categories (animate/inanimate) and 3 subcategories (animate: bird, cat, and fish; inanimate: airplane, bike, and boat), with 2 images per subcategory. Each image was cropped to 300 × 300 pixel and converted using GIMP (v 2.8, www.gimp.org) into both a two-tone black (RGB: 0,0,0) and white (RGB: 255,255,255) Mooney image (Mooney 1957; Moore and Cavanagh 1998) and a grayscale image (RGB values were situated in between black and white). All Mooney stimuli had a Michelson contrast of 1.

Experimental Procedure

The experiment was a within-subject, double-blind design consisting of 2 experimental sessions: one where a placebo and one where ketamine was administered. The order of the drug (ketamine or placebo) conditions was counterbalanced across subjects (7 subjects received placebo in the first session). The 2 experimental sessions were 2 weeks apart. Subjects were asked not to drink and eat, respectively, 3 and 6 hours prior to testing to prevent nausea.

For an overview of the experimental procedures, see Figure 1. Upon arriving subjects filled out the first of the 4 Visual Analogue Scale (VAS) measurements to assess subjective state of sedation (Bond and Lader 1974). Subjects marked a point on each scale that best indicated their state. Each scale consisted of a line (100 mm) that connected 2 opposite states of mind (e.g., “alert” and “drowsy”), where the middle, for example, 50 mm indicates a neutral state. The mean score of a subset of these scales (alert/drowsy, excited/calm, clearheaded/muzzy, energetic/lethargic, and quick/slow) was calculated for each subject and was taken as a measure of sedation (Danion et al. 1989).

This was followed by the Mooney Identification task in which subjects had to identify the Mooney images. Each Mooney image

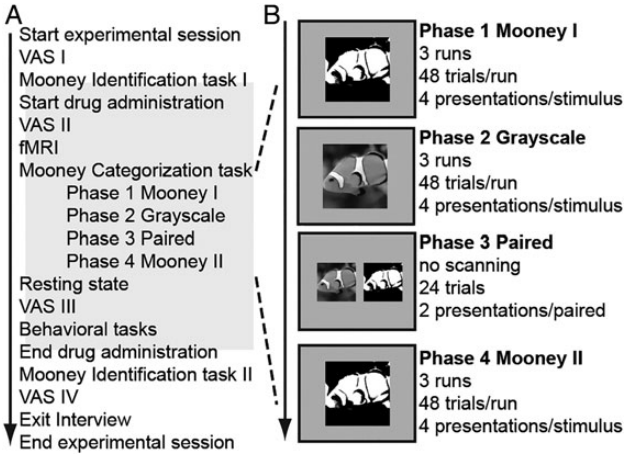

Figure 1. Overview of the experimental procedures. (*A*) Overview of the experimental session. (*B*) fMRI Mooney Categorization task: images were presented for 180 ms and participants had to indicate within 1500 ms whether the image depicted an animate or inanimate object. The task consisted of 3 fMRI phases. Each fMRI phase contained 3 runs. In each run, every stimulus was presented 4 times (48 trials in total and interleaved with fixation).

was presented once for 180 ms on the center of the computer screen. After each presentation, subjects were instructed to write down what was depicted on the image. A Viewsonic LCD screen was used with a refresh rate of 60 Hz (40 × 26° of visual angle), and stimuli were presented with Presentation (Neurobehavioral Systems).

After this task, an anesthesiologist intravenously administered the drug (placebo or a subanesthetic dose of S-Ketamine) (see Drug Administration section for details). Experimenters and subjects were blind to the drug condition. The subjects were then told to rest for 15 min during which they filled out the second VAS. After these 15 min, the subjects were led to the MRI scanner in which they participated in the fMRI Mooney Categorization task described later, followed by a resting state scan of 10 min. After fMRI recordings, subjects filled in a third VAS and performed 3 behavioral tasks, identical for each condition, that were aimed at answering research questions that are part of a separate, unrelated, study. The last and fourth VAS was taken 30 min after drug administration ended. Finally, subjects performed the same Mooney Identification task that they performed before the fMRI recordings, to assess whether the Mooney images were more easily recognized following the fMRI categorization task. Finally, an exit interview was taken, consisting of questions regarding the possible side effects of the drug administration, and to assess whether they were aware of the drug condition they were in.

In a separate session, 1 week prior to the start of the experiment, recordings were made to chart the retinotopic areas (see section on Region of interest localizers) and the subjects were informed about the overall procedure of the experiment.

Drug Administration

An anesthesiologist (aware of group allocation for safety reasons) administered the drugs via venous access that was established using a 20G intravenous catheter (Vasofix, B Braun). Subsequently, a subanesthetic dose of S-ketamine (Eurocept BV) or placebo (saline, NaCl 0.9% [B Braun]) was administered intravenously. First, a slow bolus of 0.15 mg/kg was administered followed by continuous infusion of 0.1 mg/kg/h using an infusion pump (Perfusor fm, B Braun) to keep plasma levels constant throughout the experiment.

fMRI Mooney Categorization Task

This task (see Fig. 1 for overview) consisted of 3 different fMRI phases during which the stimuli were presented: 1) Mooney I, presentation of the Mooney images, 2) Grayscale, presenting the easily identifiable grayscale photographic versions of the same images, and 3) Mooney II, during which the same Mooney images were presented as in the Mooney I phase. We expected that the prior experience with the corresponding grayscale images would make the Mooney images in the Mooney II phase easier to recognize than in the Mooney I phase. Additionally, we also presented both the grayscale and the corresponding Mooney image simultaneously side by side (Paired) after the second phase (Grayscale) to ensure recognition of the images in the Mooney II phase. Here, each pair was presented for 4 s, and was presented twice. Subjects were instructed to carefully study the association between the 2 images. No scanning was performed in this phase.

Every phase (Mooney I, Grayscale, and Mooney II) consisted of 3 event-related fMRI runs with a duration of ~5 min. A run consisted of 48 trials (all 12 stimuli were presented 4 times) and where interleaved with 99 null events with a fixation dot. Trials and null events had the same duration as the TR (2 s). We ensured that each run started and ended with at least 4 null events. The trial order was optimized using optsec2, an optimal sequencing program (NMR center, Massachusetts General Hospital). In a trial, a stimulus was presented for 180 ms and subjects had to indicate within 1500 ms after stimulus presentation whether the image depicted an animate or inanimate category. Response buttons were counterbalanced across subjects and sessions. Each run started with 10-s fixation and ended with 12-s fixation. Eye tracking data (EyeLink 1000, SR Research) was recorded to ensure fixation. The stimuli were back-projected on a 61 × 36 cm LCD screen using Presentation (Neurobehavioral Systems) and viewed through a mirror attached to the head coil, with a radius 8.4° visual angle.

Trials with a reaction time (RT) deviating more than 2 SD from the average were excluded from the behavioral analysis. Behavioral performance was compared using a repeated-measures ANOVA for drug condition (placebo and ketamine) × recognition phase (Mooney I, Grayscale, Mooney II).

fMRI Acquisition

We used a 3T Philips Achieva TX MRI scanner with a 32-element head coil. At the beginning of each session, a high-resolution 3DT1-weighted anatomical image (TR, 8.175 ms; TE, 3.74 ms; FOV, 240 × 220 × 188, 1 mm^3 voxel size, 2 averages) was recorded for each subject. During the fMRI Mooney Categorization task, we recorded Gradient-Echo, Echo Planar Imaging (GE-EPI, TR 2000 ms, TE 27.63 ms, FA 76.1°, 37 slices, voxel size 3 mm^3, slice gap 0.3 mm, FOV 240 × 121 × 240, SENSE 2).

fMRI Data Analysis

We recorded, for the fMRI Mooney Categorization task, for each subject, 9 runs of blood oxygenation level dependent (BOLD)-MRI data. We first performed motion correction on the central run and subsequently averaged these runs together. This averaged BOLD-MRI was next used for the motion correction of all runs recorded in that session. The subsequent preprocessing steps consisted of brain extraction, slice-time correction, and high-pass filtering (cutoff 100 s) using FSL (Oxford Centre for Functional MRI of the Brain (FMRIB) Software Library; www.fmrib.ox.ac.uk/fsl [Smith et al. 2004]). No spatial smoothing was applied. Anatomical scans were automatically segmented using the Freesurfer package (http://surfer.nmr.mgh.harvard.edu/) (Dale et al. 1999). BOLD-MRI data were registered to the subject-specific T1 scan using boundary-based registration (Greve and Fischl 2009). The subject-specific T1 scan was registered to the MNI brain using FMRIB's Nonlinear Image Registration Tool.

Every phase of a session (Mooney I, Grayscale, and Mooney II) consisted of 3 event-related fMRI runs in which 12 stimuli were presented 4 times. For each subject and each run, a general linear model was fitted to the data, where every stimulus (4 presentations) was convolved with a standard HRF and taken as a regression variable. We computed the *t*-values by dividing the resulting beta weight for each predictor (effect of stimulus presentation compared with the baseline) with the standard error. Time-series statistical analysis was carried out using FILM (Woolrich et al. 2001). The data were further analyzed in Matlab (The MathWorks). For every participant, we created per ROI a vector containing the *t*-value per voxel for each stimulus. That vector comprised the spatial pattern of activity evoked by that stimulus. We averaged these patterns over runs per subject per condition.

Next, we used these patterns to answer the question whether the Mooney II stimuli resemble the Mooney I or Grayscale stimuli more. To determine this, we used a soft-margin Support Vector Machine (SVM) classifier using a linear kernel with parameter C set to 1 (Bioinformatics Toolbox, Matlab). The parameter C controls a tradeoff between the strictness of the decision rule and allowed errors during the training procedure. With $C = 1$, no training error is allowed, which is recommended for small sample sizes and high-dimensional data. Before training, the data were scaled using a z-transformation. In brief, an SVM calculates a hyperplane during a training phase, which optimally separates between 2 classes of presented training data. Here, we used the vector of t-values per voxel, that is, the activity patterns from the Mooney I phase and the Grayscale phase as the 2 classes in the training data. Next, we tested as which of these phases the stimuli from the Mooney II phase were classified. This yielded a classification score (percentage Mooney II images classified as grayscale) per subject per ROI for every condition (drug and recognition).

Additionally, to assess and visualize how recognition affected the neural representations of individual images within a recognition phase, we created for each run of every experimental condition (drug [placebo and ketamine] and recognition [Mooney I, Grayscale, and Mooney II]), a representational dissimilarity matrix (RDM) (Kriegeskorte et al. 2008). An RDM is a symmetric square matrix and a simple method to visualize the differences between activation patterns of stimuli. Each cell of the matrix represents a 1-r (Pearson correlation) of the activity patterns of 2 stimuli (0 for perfect correlation, 1 for no correlation, and 2 for perfect anti-correlation). We averaged the RDMs of all runs, to obtain a single RDM per condition.

To assess whether ketamine affected the hemodynamic BOLD response, we performed a deconvolution analysis to estimate the time course of the BOLD response (Glover 1999). This was done separately for each drug condition, each subject, and for area V1 and pFs. The preprocessed time series were z-transformed, up-sampled by a factor of 2 (from 2 s (TR) to 1 s) and averaged per run. Deconvolution was performed on a time window of 4 s before and 20 s after stimulus presentation, using all stimulus presentations (48 per run) as predictors. Finally, we computed the mean BOLD response time course and SEM across subjects per drug condition and tested with a repeated-measures ANOVA and paired-tests whether the drug condition differed in their hemodynamic BOLD response.

Region of Interest Localizers

Visual areas were localized using an eccentricity mapper (2 runs) and a polar angle mapper (6 runs). The eccentricity mapper consisted of a checkerboard ring (red-green tiles, flickering at 6 Hz) expanding from center to periphery (1 run) and contracting from periphery to center (1 run). The polar angle mapper was a checkerboard wedge (red-green tiles, flickering at 6 Hz) rotating around fixation (3 clockwise and 3 counterclockwise runs). Subjects were instructed to fixate at the center while detecting blue color changes of the checkerboard tiles.

For these mappers, a gradient-echo, echo-planar pulse sequence was used (TR 2000 ms [Polar] TR 2500 ms [Eccentricity], TE 27.63 ms, FA 76.1°, 24 slices with ascending acquisition, voxel size 2.5 mm^3, slice gap 0.25 mm, FOV 66 × 200 × 144) centered on the calcarine sulcus.

The polar angle and eccentricity localizers allowed us to define visual areas (V1, V2, V3, and V4). For each subject, data of these localizers were projected onto an inflated surface reconstruction of the subject's brain (using Brainvoyager 2.1 [Brain Innovation {Goebel et al. 2006}]). The end result of the region of interest analysis in Brainvoyager resulted in regions of interest in Talairach space. The regions of interest were first transformed from Talairach space to the subject specific, AC-PC aligned, T1 scan. This scan was then used for determining the transformation to MNI space. We subsequently used this transformation to transform the subject-specific regions of interest to MNI space.

The lateral occipital complex (LOC) was mapped using the region that responded more strongly to intact versus scrambled objects (Malach et al. 1995). We selected voxels within the posterior fusiform part of LOC using an anatomical mask of the temporal occipital fusiform cortex (from the Harvard-Oxford Cortical Structural Atlas of the FSL package) since this region is generally known to be category selective and involved in the high-level processing of visual objects. We will refer to this region as pFs. Stimuli were presented for 300 ms and consisted of 20 intact and 20 scrambled objects that were presented in separate blocks (16 in total). Subjects were asked to push a button when 2 consecutive images were identical. For this mapper, BOLD-MRI was recorded using Echo Planar Imaging (EPI) (TR 2000 ms, TE 27.63 ms, FA 76.1°, 37 slices with ascending acquisition, voxel size 3 mm^3, slice gap 0.3 mm, FOV 240 × 121 × 240).

The same preprocessing steps as described for the fMRI Mooney Categorization task were performed for the LOC mapper. To combine the 2 runs for each subject, we used a fixed-effects analysis (Beckmann et al. 2003).

Results

Behavioral Results

Sedation

Two subjects were excluded due to repeatedly falling asleep and low vigilance during scanning in the ketamine condition resulting in too many missing trials (> 85 trials, >2 standard deviations from the mean) in specific recognition phases. Subjective sedation scores were compared using a repeated-measures ANOVA for drug condition (placebo and ketamine) × time (4 levels) and post hoc paired t-tests (false discovery rate [FDR] corrected) on the remaining participants. We observed a significant interaction between drug and time ($F_{3,36} = 17.63$, $P = 0.0000003$). Before the start of the experiment and drug administration, there was no difference between placebo and ketamine ($t_{1,14} = 0.186$, $P = 0.855$). Participants felt more sedated on ketamine than on placebo, after the bolus injection ($t_{1,13} = 5.27$, $P = 0.0002$) and right after the fMRI Mooney Categorization task ($t_{1,13} = 3.02$, $P = 0.010$) as measured with the VAS (see Fig. 2A). This effect was no longer significant 30 min after ending the drug administration ($t_{1,14} = 2.17$, $P = 0.048$). Our drug manipulation therefore seemed to be of a sufficient dose to induce behavioral sedative effects.

Mooney Identification Task before and after Scanning

Next, to test whether the Mooney images were not recognized initially but recognized following the fMRI Mooney Categorization task, subjects had to identify what was depicted in the Mooney images at the start and at the end of the experimental session (see Fig. 2B). An answer was regarded as correct if participants wrote down the superordinate category of the object (animal or vehicle). We observed no interaction effect ($F_{1,14} = 1.07$, $P = 0.319$) or a main effect of drug condition ($F_{1,14} = 0.88$, $P = 0.363$). There was a main effect for recognition on the Mooney Identification task ($F_{1,14} = 440.67$, $P = 0.0000001$); participants were better at

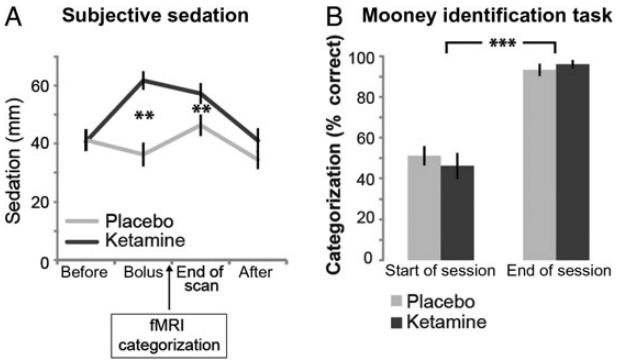

Figure 2. Subjective sedation and behavioral results. (A) Subjective state of sedation. Ketamine administration induced subjective sedation. Subjects felt more sedated on ketamine than on placebo, after the bolus injection and right after the fMRI Mooney Categorization task as measured with the VAS. This effect was no longer significant 30 min after drug administration. Our drug manipulation therefore seemed to be of a sufficient dose to induce behavioral sedative effects. (B) Results for the Mooney identification task. Participants identified more Mooney images at the end of the session ("after") than before the scanning ("before"), no difference between the drug conditions. Error bars indicate SEs; **P FDR corrected, ***P < 0.001.

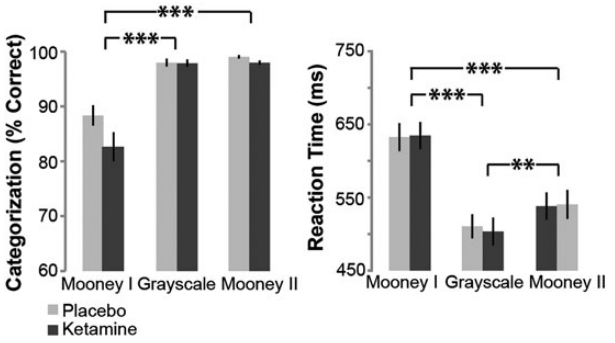

Figure 3. Behavioral results of fMRI Mooney Categorization task. Categorization between animate and inanimate objects was better and faster when subjects were able to recognize what was depicted in the image (Grayscale and Mooney II) than before recognition (Mooney I), as reflected both in categorization performance and in RT. Ketamine slightly reduced the categorization performance for the recognized Mooney images (Mooney II) compared with placebo. Error bars indicate SEs; **P FDR corrected, ***P < 0.001.

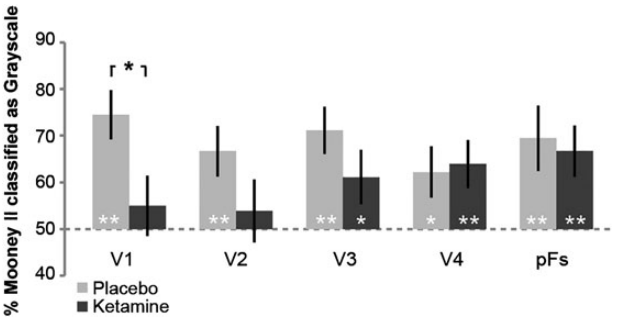

Figure 4. Classification performance for all ROIs. In the placebo condition, the images in the Mooney II phase were classified more as their counterpart grayscale images than as the images before recognition in the Mooney I phase in all ROIs. In the ketamine condition, this effect of recognition disappeared in V1 and V2. Error bars indicate SEs; *P < 0.05, **P FDR corrected.

categorizing what was depicted on the Mooney images at the end of a session than before.

fMRI Mooney Categorization Task

In the scanner, subjects performed the fMRI Mooney Categorization task during all recognition phases (Mooney I, Grayscale, and Mooney II). Here, subjects had to indicate via button presses whether the depicted object in the image was animate or inanimate. Behavioral performance was compared using a repeated-measures ANOVA for drug condition (placebo and ketamine) × recognition phase (Mooney I, Grayscale, and Mooney II) and tested with post hoc paired *t*-test (false discovery rate (FDR) corrected). We did not observe significant interactions between drug condition and recognition phase for RT ($F_{1,14} = 0.01$, $P = 0.928$) and for percentage correct ($F_{1,14} = 2.07$, $P = 0.145$). Nor did we find a main effect of drug condition (RT: $F_{1,14} = 0.01$, $P = 0.928$, percentage correct: $F_{1,14} = 3.25$, $P = 0.093$). But, as expected subjects were better and faster in judging category in the Grayscale phase and Mooney II phase than in the Mooney I phase (main effect for recognition phase, Percentage Correct: $F_{2,28} = 74.86$, $P = 0.0000001$ and RT: $F_{2,28} = 60.58$, $P = 0.0000001$, see Figure 3 for results). The recognition of the Mooney images (Mooney II) increased the categorization performance as compared with Mooney I (all $t_{1,14} > 5.49$, $P < 0.00008$), and categorization performance did not differ from performance in the Grayscale phase (all $t_{1,14} < 1.63$, $P > 0.126$). Subjects had the shortest RTs for the grayscale images (all $t_{1,14} > 3.34$, $P < 0.005$). Our behavioral results thus show that due to the prior experience with the grayscale images, the performance in the Mooney II phase resembled that of the performance in the Grayscale phase. Ketamine administration, however, had no effect on behavioral performance. These results show that participants under ketamine administration were still able to perform the task properly although participants reported to feel more sedated in this condition.

fMRI Results

Classification

Next, we wanted to test the effect of recognition and ketamine on neural object representations. Based on a study by Hsieh et al. (2010), we hypothesized that neural representations of recognized Mooney images should resemble the representation of their counterpart grayscale photos more than that of identical unrecognized Mooney images, both in pFs and V1. To test this, we trained a neural pattern classifier on the multivoxel patterns elicited during the Mooney I phase and Grayscale phase. Next, we used this classifier to categorize the multivoxel patterns obtained during the Mooney II phase as either corresponding to the Mooney I or to the Grayscale phase. Based on a previous study by Hsieh et al. (2010), we predicted that the Mooney II representations would be classified more as Grayscale than as Mooney I. First, we performed one-sample *t*-tests (FDR corrected) to investigate whether this classification performance was above 50% (indicating classified as grayscale) for all ROIs and drug condition (see Fig. 4). In the placebo condition, we observed for all ROIs (trending for V4: $t_{1,14} = 2.24$, $P = 0.042$) that images in the Mooney II phase were classified more often as grayscale images than as Mooney images before recognition (Mooney I phase) (all $t_{1,14} > 2.79$, $P < 0.015$). This suggests that representations in early visual areas reflect an integration of bottom-up input and top-down interpretation. Interestingly, however, during ketamine, classification was only above chance in area V4 and pFs (all $t_{1,14} > 2.71$, $P < 0.017$). Next, to assess the difference between ketamine and placebo and ROIs, we ran a repeated-measures ANOVA with

drug (placebo and ketamine) and ROI (V1, V2, V3, V4, and pFs). Since we expected that ketamine would mainly interfere in early visual areas, we used a Helmert contrast analysis for ROI. We only found an interaction effect between drug condition and ROI (V1 vs. V2, V3, V4, and pFs) ($F_{1,14} = 5.291$, $P = 0.037$, see Fig. 4). A post hoc paired *t*-test comparing the difference between placebo and ketamine in V1 resulted in a trend ($t_{1,14} = 2.26$, $P = 0.040$). Implying that the classification performance difference between ketamine and placebo was largest in V1 compared with the other ROIs.

In order to address the alternative hypothesis that these results may have been caused by nonspecific effects of ketamine such as sedation, we correlated the subjective sedative measure with the classification accuracy in V1. It is unlikely that these results in V1 can be attributed to sedation, since we find a negative correlation between sedation (ketamine minus placebo sedation score, rated at bolus and at the end of the task with the VAS) and classification accuracy. As a result, the participants who felt most sedated displayed the smallest difference between ketamine and placebo in classification performance (Rho = –0.552, $P = 0.033$).

In sum, these results suggest that image recognition changes neural representations in early visual areas and that ketamine interferes with this process.

Representational Dissimilarity Matrices

To further identify the nature of this change, we looked at the dissimilarity between individual neural object representations within each recognition phase. We created representational dissimilarity matrices (RDM) for each recognition phase, drug condition, and region of interest. Next, we computed the mean dissimilarity for each condition by averaging all the cells within an RDM to compare overall dissimilarity between conditions (see Fig. 5). For V1 and pFs, the mean dissimilarity of each RDM was used as input in a repeated-measures ANOVA with 2 factors: recognition phase (Mooney I, Grayscale, and Mooney II) and drug condition (placebo and ketamine) and tested with post hoc paired *t*-test (FDR corrected).

Using RDMs, Kriegeskorte et al. (2008) have shown that in object-related areas spatial patterns from objects within the same category are more similar than between category patterns. In this study, however, we will not report these category-selective

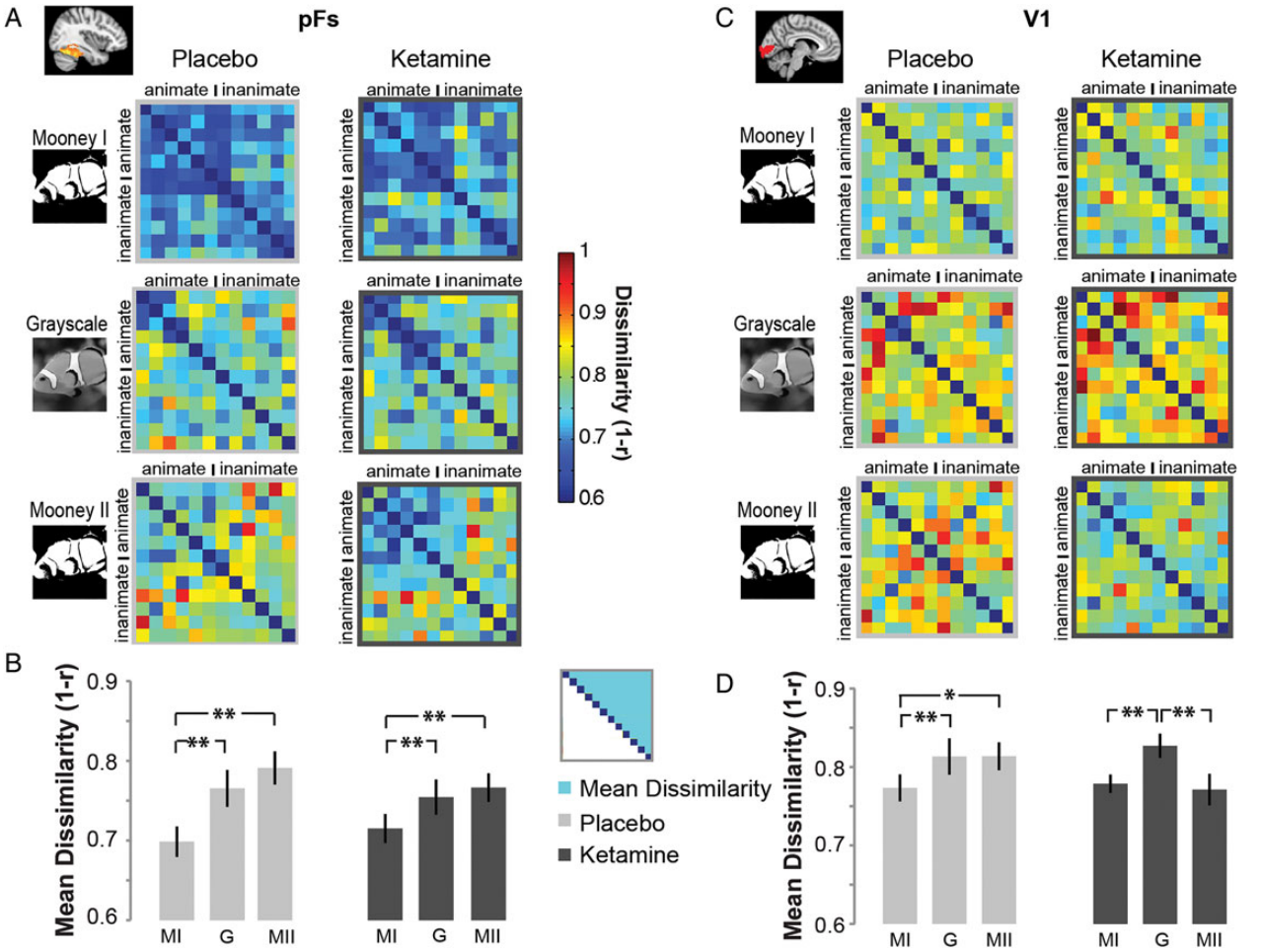

Figure 5. RDMs and mean dissimilarity in pFs and V1. (*A*) RDMs for each drug condition (Left: placebo, right: ketamine) and recognition phase (top to bottom: Mooney I, Grayscale, and Mooney II) for pFs. The color coding represents the amount of dissimilarity in the pFs-activation patterns between 2 stimuli, where blue indicates stimuli being similar and red dissimilar. (*B*) Mean dissimilarity in pFs. Recognition altered the dissimilarity between the neural representations of images. Dissimilarity was lowest for the unrecognized Mooney images. (*C*) RDMs for V1. (*D*) Mean dissimilarity for V1. Object recognition (Grayscale and Mooney II) increased the mean dissimilarity as compared with before recognition (Mooney I). However, in the ketamine condition, dissimilarity was reduced for the recognized Mooney images (Mooney II); Mooney I and Mooney II did not differ. Error bars indicate SEs; *$P < 0.05$, **P FDR corrected.

responses since it was not the main focus of this study. But, we would like to point out that we did not observe any effect of ketamine on these category-selective responses in pFs.

We predicted that recognition should alter the dissimilarity between neural object representations. In pFs, there was no interaction between drug intake and recognition on mean dissimilarity ($F_{1,14} = 1.43$, $P = 0.256$) and no main effect of drug intake on mean dissimilarity ($F_{1,14} = 0.14$, $P = 0.713$). But, there was a main effect of recognition ($F_{2,28} = 21.16$, $P = 0.000003$). Object recognition changed the mean dissimilarity in pFs; neural object representations became more dissimilar with recognition (see Fig. 5A,B). First, dissimilarity between the object representations was higher for the grayscale images than that for the unrecognized Mooney images (Mooney I): placebo ($t_{1,14} = 3.19$, $P = 0.007$) and ketamine ($t_{1,14} = 3.02$, $P = 0.009$). Importantly, we also observed this for the Mooney II phase; after recognition (Mooney II) dissimilarity increased compared with before recognition (Mooney I): placebo ($t_{1,14} = 5.82$, $P = 0.000045$) and ketamine ($t_{1,14} = 2.74$, $P = 0.016$). Furthermore, we found no difference in mean dissimilarity between Grayscale and Mooney II: placebo ($t_{1,14} = 1.68$, $P = 0.114$) and ketamine ($t_{1,14} = 0.73$, $P = 0.476$). Thus, having prior experience with the grayscale images changed the neural representations of the Mooney images, making them more differentiated from each other. Before recognition, Mooney images "look more alike" from a neural perspective. Recognition makes their neural representations more differentiated. The NMDA receptor did not seem to play a role in this effect in pFs since there was no effect of ketamine.

Interestingly, in V1, ketamine administration did influence the neural representations (see Fig. 5C,D). Since we expected that ketamine would mainly interfere with Mooney II phase, we used a Helmert contrast for recognition phase to test the interaction with drug treatment. Indeed, we observed a significant interaction effect ($F_{1,14} = 6.21$, $P = 0.026$, Mooney II vs. Grayscale and Mooney I). Additional post hoc paired t-tests (FDR corrected) revealed that in the ketamine condition mean dissimilarity did not differ between the Mooney I phase and Mooney II phase ($t_{1,14} = 0.38$, $P = 0.708$) whereas they did significantly differ from the Grayscale phase ($t_{1,14} = 2.71$, $P = 0.017$). These results indicate that with ketamine, the prior experience with the grayscale images did not change the neural representations of Mooney images in the Mooney II phase, whereas they do change with placebo. Here, mean dissimilarity in the Mooney II phase seemed increased compared with Mooney I phase (trend: $t_{1,14} = 2.26$, $P = 0.041$) and Grayscale and Mooney II did not differ ($t_{1,14} = 0.46$, $P = 0.654$), whereas Grayscale and Mooney I did ($t_{1,14} = 2.50$, $P = 0.026$). Again, it is unlikely that the effects of ketamine can be attributed to sedation or lower signal-to-noise ratio (SNR). The representational dissimilarity between the Mooney II and other phases was higher in the placebo than that in the ketamine condition. The specificity of this effect (pertaining specifically to Mooney II, rather than a general difference across all conditions) shows that it cannot be accounted for by nonspecific effects of ketamine. In addition, the ketamine effect was specific to V1; we did not observe a ketamine effect in pFs, further strengthening the case against nonspecific sedative or SNR effects. Finally, we did not find a correlation between differences in sedation and differences in dissimilarity during the Mooney II phase (Rho = 0.061, $P = 0.830$).

Thus, V1 results for the placebo condition seemed very similar to those in pFs; object recognition increased the dissimilarity between images, making the neural representations more distinguishable. However, ketamine interfered with the Mooney recognition effect in V1; prior experience with the grayscale images did not alter the mean dissimilarity in the Mooney II phase.

Additionally, we were interested whether the effect of recognition and ketamine varied across region of interest and drug condition. Therefore, we ran similar analyses for areas V2, V3, and V4. To assess the recognition effect, we computed the difference in the mean dissimilarities between the Mooney I and Mooney II phase as well as between the Mooney II and Grayscale phase. First, we used one-sample t-tests (FDR corrected) to test whether the recognition phases differed from each other for V2, V3, and V4 (Fig. 6A). In the placebo condition, the Mooney II phase and Mooney I phase were significantly different in all visual regions as assessed with one-sample t-tests (all $t_{1,14} > 3.24$, $P < 0.006$). In the ketamine condition, this significant difference was present only in areas V3 and V4 (all $t_{1,14} > 2.29$, $P < 0.018$) and not in V2; recognition did not increase the mean dissimilarity here (V2: $t_{1,14} = 0.71$, $P = 0.487$). We did not find a significant differences between the Mooney II and Grayscale phase in V2, V3, and V4 for placebo or ketamine (all $t_{1,14} < 1.04$, $P > 0.315$, see Fig. 6B). In order to test whether the ketamine condition differed significantly from the placebo condition and how this effect varied across region of interest, we ran for both the subtractions (Mooney II–Mooney I and Mooney II–Grayscale) a repeated-measures ANOVA using drug condition (placebo and ketamine) and ROI using a Helmert contrast (V1 V2, V3, V4, and pFs). We did find a significant interaction for the Mooney II–Grayscale but only with the Helmert contrast V1 versus V2, V3, V4, and pFs ($F_{1,14} = 4.83$, $P = 0.045$); using a post hoc paired t-test, we directly confirmed a significant difference between the placebo and the ketamine conditions in V1 ($t_{1,14} = 2.59$, $P = 0.021$). These results suggest that only in V1, ketamine disturbed the effect of Mooney recognition, since the mean dissimilarity did differ from the Grayscale phase. However, for the Mooney II–Mooney I, we did not found a significant interaction (all $Fs_{1,14} < 1.316$, all $P = 0.875$) or main effect for drugs ($F_{1,14} = 1.87$, $P = 0.193$). Therefore, we

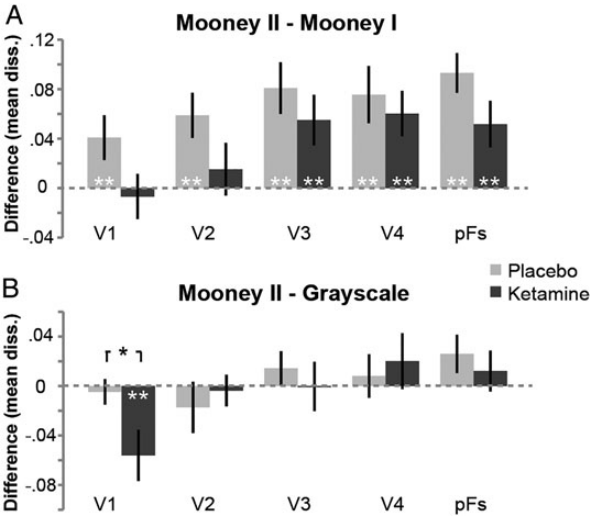

Figure 6. Difference in mean dissimilarity for areas V1, V2, V3, V4, and pFs. (*A*) Difference between the recognized (Mooney II) and unrecognized Mooney (Mooney I) phase. In the ketamine condition, the mean dissimilarity in areas V1 and V2 did not differ before and after the presentation of the grayscale images. In the placebo condition and in areas V3, V4, and pFs, the mean dissimilarity did increase with recognition. (*B*) Difference between Mooney II and Grayscale phase. Ketamine seemed to specifically interfere in V1; mean dissimilarity did not increase in the Mooney II phase compared with the Grayscale phase. Whereas on the other ROIS and in the placebo condition, there was no difference between Mooney II and Grayscale. Error bars indicate SEs; *$P < 0.05$, **P FDR-corrected.

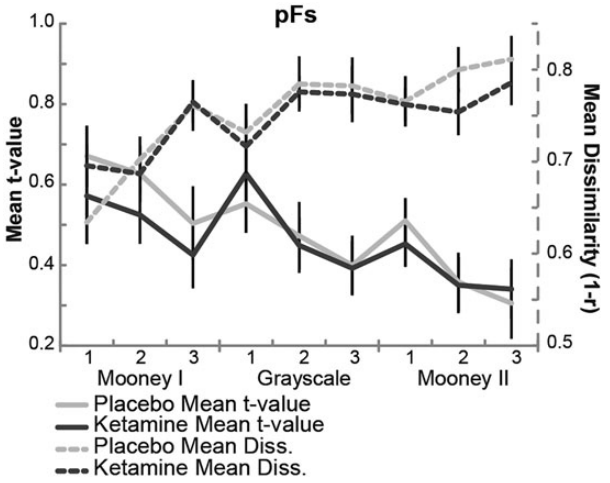

Figure 7. Mean response and mean dissimilarity over runs in pFs. Both in the placebo and ketamine condition, mean response decreased and mean dissimilarity increased in pFs. Error bars indicate SEs.

Table 1 Pearson correlations between mean response and mean dissimilarity

	V1	V2	V3	V4	pFs
Placebo	−0.380*	−0.293*	−0.459*	−0.493*	−0.719*
Ketamine	−0.113	−0.120	−0.208*	−0.461*	−0.623*

Note: In the placebo condition, mean response correlated negatively with mean dissimilarity in all ROIs. In the ketamine condition, we only observed this negative correlation in areas V3, V4, and pFs and not in areas V1 and V2 (*P FDR corrected).

cannot conclude that the mean dissimilarity in the Mooney II phase remained the same as before recognition for V1 in the ketamine condition. We did observe a main effect for ROI ($F_{4,56}$ = 6.48, P = 0.00023), implying that the dissimilarity difference between Mooney II and Mooney I increased from V1-pFs. Again, the differences in sedation did not correlate with differences between ketamine and placebo in V1 (Mooney II–Mooney I: Rho = 0.100, P = 0.723 and Mooney II–Grayscale: Rho = –0.264, P = 0.341).

Together, our results demonstrate that object recognition changes neural object representations in early visual areas and pFs. Ketamine seemed to interfere with this process in V1 since the Mooney II phase representations still differed from the Grayscale phase.

Importantly, this ketamine effect could not be explained by a difference in mean response. As an index of mean response, we calculated the mean t-values for each drug condition and recognition phase and observed no effect of drug condition: V1 ($F_{1,14}$ = 0.756, P = 0.399) and pFs ($F_{1,14}$ = 1.16, P = 0.300). We did, however, observe a relation between mean response and mean dissimilarity in pFs; the mean response decreased over runs ($F_{8,112}$ = 7.19, P = 0.0000001) and mean dissimilarity increased linearly over runs ($F_{8,112}$ = 9.83, P = 0.0000001, see Fig. 7).

To investigate this relationship further, we ran an additional post hoc analysis where we correlated every mean response and mean dissimilarity for each run and every participant (see Table 1). We indeed found a negative correlation between mean dissimilarity and mean response; for the placebo condition in all ROIs (all Pearson's r > 0.293, P < 0.001) and for the ketamine condition only in V3, V4, and pFs (all Pearson's r > 0.298, P < 0.015) and not in V1 and V2 (all Pearson's r < 0.120, P > 0.12). These results show that although mean responses decrease with recognition the specificity of neural object representations increases and that ketamine interfered with this process.

Deconvolution Analysis

Finally, we wanted to exclude the possibility that our results could be attributed to a general difference in the hemodynamic (BOLD) response between the placebo and ketamine condition. Therefore, we performed a deconvolution analysis to estimate the time course of the BOLD response (Glover 1999) (see Materials and Methods). We performed a repeated-measures ANOVA on the deconvolved BOLD response time course with drugs (placebo and ketamine) and time points (24 in total) as factors, separately for V1 and pFs. The hemodynamic response did not differ between ketamine and placebo (see Fig. 8); we did not observe a significant interaction between drug and time (V1: $F_{23,322}$ = 0.856, P = 0.658, pFs: $F_{23,322}$ = 0.590, P = 0.935) or main effect for drug (V1: $F_{1,14}$ = 0.121, P = 0.733, pFs: $F_{1,14}$ = 0.326, P = 0.577). Additional post hoc paired t-tests on each time point did not reveal significant differences either. This suggests that our results could not be explained by some general effect that ketamine administration may have on the hemodynamic response.

Discussion

The aim of this study was to investigate the effect of ketamine (a noncompetitive NMDA antagonist) in shaping neural object representations with recognition. First, object recognition changed neural object representations rendering them more dissimilar. In other words: from the neural perspective, unrecognizable Mooney images "all look the same" and different neural representations only arise upon recognition. More specifically, neural representations of Mooney images were classified more as the grayscale photo version of the same images when subjects knew what the Mooney images represented than when they did not. We observed these results both in pFs and early visual areas. More interestingly, ketamine interfered with these object recognition effects in V1. After ketamine intake, neural classification performance dropped and the neural representations of the Mooney images remained more similar even after having prior experience with the grayscale images. Ketamine had no effects on the behavioral categorization performance.

Taken together, the ketamine results were specific regarding location (ketamine only affected V1 not pFs), recognition phase (ketamine only affected the Mooney II phase and not the Mooney I and Grayscale), and neural effect (ketamine only influenced the neural representations and not the mean activity or hemodynamic response). Therefore, our results could not be attributed to a more general sedative effect of ketamine. Moreover, our neural ketamine effects and sedation scores did not correlate positively. We interpret our results as a demonstration that ketamine administration affects top-down processes, in turn influencing activity patterns in early visual cortex, possibly via the NMDA pathway.

This is in line with the idea that visual perception is not a simple cascade of feedforward steps, but a dynamic interplay between higher-level and lower-level areas; the higher visual areas rapidly extract the global structure of an image and can then feedback these interpretations as priors to the lower visual areas thereby changing the representations (Rao and Ballard 1999; Hochstein and Ahissar 2002; Lee and Mumford 2003; Friston

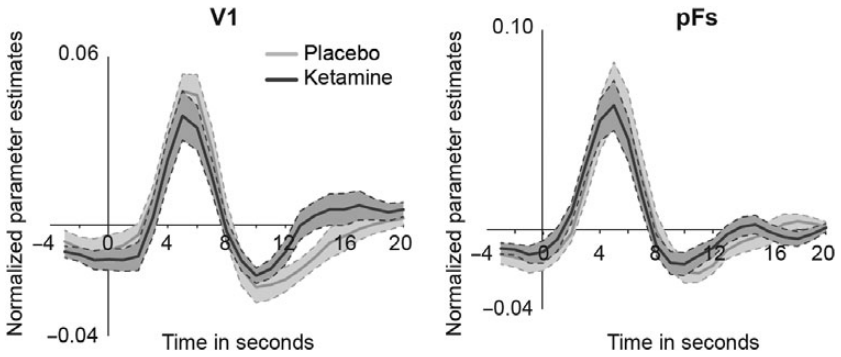

Figure 8. Deconvolution analysis of the fMRI response in V1 and pFs. We did not observe any significant differences in the fMRI response between the ketamine and placebo condition in pFs or in V1. This suggests that the observed ketamine results cannot be attributed to a difference in the fMRI response. The thick lines indicate the mean, and the thin lines indicate the SEM across subjects.

2005; Bar et al. 2006; Lamme 2006; Yuille and Kersten 2006; Summerfield and Koechlin 2008). An alternative explanation for our results includes the possibility of changes in visual spatial attention. For example, with an unrecognizable Mooney image, spatial attention is presumably uniformly distributed. In a recognizable Mooney image, spatial attention could be spatially directed at important parts of the image. But still, such attentional allocation requires high-level information and could therefore be considered as a top-down process. Indeed, attention to specific spatial coordinates has been suggested as the mechanism driving identification of object parts in Mooney face stimuli (McKeeff and Tong 2007) and figure-ground segregation (Poort et al. 2012), although it has also been shown that category-selective responses can occur independently from spatial attention (Peelen et al. 2009). Whether ketamine intake affects spatial attention or whether it affects feature representation itself remains an issue for future investigations.

The role of the NMDA receptor in top-down processes has been suggested in modeling studies (Lumer et al. 1997; Dehaene et al. 2003) and is supported with electrophysiological recordings in monkeys also using NMDA receptor antagonists (Self et al. 2012; Herrero et al. 2013). Interestingly, Herrero et al. (2013) reported that NMDA blockade in V1 selectively reduced reliability of responses by interfering with attention-induced reduction of noise correlation and attention-induced variance reduction. This seems in line with the ketamine-induced changes observed in this study; we observed that ketamine distorted the neural effects of recognition and the relationship between mean dissimilarity and mean response in V1.

Others have also observed effects of top-down manipulations on sensory processing. When, for example, top-down activity was manipulated using transcranial magnetic stimulation it was found that figure-ground modulation (Wokke et al. 2012), categorization of natural scenes (Koivisto et al. 2011), visual motion prediction (Vetter et al. 2013), and perceptual completion of Kanisza illusory contours (Wokke et al. 2013) were disturbed. Moreover, another study with ketamine demonstrated disrupted feature integration (Meuwese et al. 2013). Our results are in line with a study that used the same paradigm (Hsieh et al. 2010). They showed that the neural pattern of a Mooney image correlated more strongly with the neural pattern of the corresponding grayscale image when recognized than when not, both in pFs and in V1. However, the observed reduced mean response for the recognized Mooney images versus unrecognized Mooneys seems contradictory with previous studies, where higher mean response for recognized versus unrecognized Mooney images was found in pFs (McKeeff and Tong 2007; Imamoglu et al. 2012). But, in these studies, subjects were instructed to freely view the image and to report the time of recognition as soon as they recognized the object. In the current study, we presented 12 images very shortly (180 ms) in 3 recognition phases and the task was to categorize the images. Interestingly, we observed a relationship between mean response and mean dissimilarity. The more dissimilar the neural representations were the lower the mean response, suggesting a sharpening of responses. We observed this in pFs but also in early visual areas and found that ketamine distorted this relationship in V1/V2. Sharpening of stimulus representations in V1 has been found previously, namely for perceptual expectations (Kok et al. 2012). Our results add that the NMDA receptor could be involved in this sharpening in early visual cortex, since ketamine distorted the correlation between mean dissimilarity and mean response in V1/V2.

The current experiment was specifically designed to target feedback to early visual areas, and our effects of ketamine administration were most profound in V1. But, the effect of ketamine and/or NMDA receptor blocking is probably not only instrumental in feedback to V1. Assuming that the top-down signal from pFs needs to travel through other visual areas before it reaches V1, ketamine should also have reduced the signal in these other areas (e.g., V2). We find significantly strong effects only in V1, but our results hint of effect in other early visual areas as well (e.g., Figs 4 and 6). Maybe with a higher dose ketamine would have had more profound effects in these other visual areas as well. Although NMDA receptors are the primary target for ketamine, ketamine has a complex pharmacological profile and it exerts some additional effects on other signaling pathways and receptors (Kocsis et al. 2013). Those interactions may also contribute to the observed effects. However, in the current study, we used a dose (0.1 mg/kg), where ketamine seems to be a relatively selective and potent antagonist of the NMDA receptor (Chizh 2007; Kotermanski et al. 2013). Further research could use different tasks and NMDA receptor antagonists to investigate the role of NMDA in feedback to visual areas more specifically.

Additionally, we would like to note that the NMDA receptor is probably not the only important receptor in top-down processes. For instance, recordings of single cell activity in monkeys demonstrated reduced attentional feedback in V1 with scopolamine, a muscarine antagonist (Herrero et al. 2008). The role of GABA in top-down processing has been shown in an experiment where the $GABA_A$ receptor agonist lorazepam impaired figure-ground modulation in humans (van Loon et al. 2012). Additionally, recordings in macaque monkeys anesthetized with isoflurane

demonstrated suppressed top-down processing (Lamme et al. 1998). Isoflurane not only binds to NMDA but also to GABA and glycine receptors. We know that anesthetics act on many different neurotransmitter systems apart from NMDA, such as GABA, Glycine, and Acetylcholine (for a review, see Alkire et al. (2008). Anesthetics operate by disrupting the balance between excitation and inhibition (Alkire et al. 2008). Some suggest that blockage of the NMDA receptor could be the final common pathway of many anesthetic drugs (Flohr et al. 1998), but it is more likely that anesthetics operate by disrupting the balance between excitation and inhibition (Alkire et al. 2008), which in turn affects recurrent or top-down processing (Roelfsema et al. 2002; Ferrarelli et al. 2010; Wyatte et al. 2012). But, the role of these other receptors in top-down processing should be investigated further.

We did not find a behavioral effect of our ketamine manipulation. This could suggest that categorization performance was mainly driven by pFs representations. This is in line with the idea that categorization can occur based on feedforward activity, whereas more detailed feature extraction requires top-down activation of early visual areas (Hochstein and Ahissar 2002; Fahrenfort et al. 2012). This may have been revealed with a task focusing on details of the image instead of their global category. Or maybe with a higher dose a behavioral effect could have been induced. For example, a study that used different doses of ketamine in Monkeys observed no effect at a low-dose (comparable to our study) but did find performance deficit with higher doses on a perceptual delayed-match-to-sample task (Taffe et al. 2002). Further research could test the effects of different doses of ketamine.

In sum, we demonstrated that object recognition sharpens the neural representations of objects. This effect was observed both in pFs and in early visual areas. Interestingly, ketamine reduced the effect of recognition in V1. Therefore, activity patterns in V1 not simply reflect sensory input but are reshaped by top-down processes, which are possibly mediated by the NMDA pathway.

Funding

This work was supported by Advanced Investigator Grant 230355 from the European Research Council to V.A.F.L.

Notes

We thank the volunteers for their participation and Simon van Gaal for helpful advice. *Conflict of Interest*: None declared.

References

Albers AM, Kok P, Toni I, Dijkerman HC, de Lange FP. 2013. Shared representations for working memory and mental imagery in early visual cortex. Curr Biol. 23:1427–1431.

Alkire MT, Hudetz AG, Tononi G. 2008. Consciousness and anesthesia. Science. 322:876–880.

Bar M, Kassam KS, Ghuman AS, Boshyan J, Schmid AM, Dale AM, Hämäläinen MS, Marinkovic K, Schacter DL, Rosen BR, et al. 2006. Top-down facilitation of visual recognition. Proc Natl Acad Sci USA. 103:449–454.

Beckmann CF, Jenkinson M, Smith SM. 2003. General multilevel linear modeling for group analysis in FMRI. NeuroImage. 20:1052–1063.

Bond A, Lader M. 1974. The use of analogue scales in rating subjective feelings. Br J Med Psychology. 47:211–218.

Chizh BA. 2007. Low dose ketamine: a therapeutic and research tool to explore N-methyl-D-aspartate (NMDA) receptor-mediated plasticity in pain pathways. J Psychopharm. 21:259–271.

Dale AM, Fischl B, Sereno MI. 1999. Cortical surface-based analysis: I. Segmentation and surface reconstruction. NeuroImage. 9: 179–194.

Danion J-M, Zimmermann M-A, Willard-Schroeder D, Grange D, Singer L. 1989. Diazepam induces a dissociation between explicit and implicit memory. Psychopharmacology. 99:238–243.

Dehaene S, Sergent C, Changeux J-P. 2003. A neuronal network model linking subjective reports and objective physiological data during conscious perception. Proc Natl Acad Sci USA. 100:8520–8525.

Ekstrom A, Kahana M, Caplan J, Fields T, Isham E, Newman E, Fried I. 2003. Cellular networks underlying human spatial navigation. Nature. 425:184–188.

Fahrenfort JJ, Snijders TM, Heinen K, van Gaal S, Scholte HS, Lamme VAF. 2012. Neuronal integration in visual cortex elevates face category tuning to conscious face perception. Proc Natl Acad Sci USA. 109:21504–21509.

Ferrarelli F, Massimini M, Sarasso S, Casali A, Riedner BA, Angelini G, Tononi G, Pearce RA. 2010. Breakdown in cortical effective connectivity during midazolam-induced loss of consciousness. Proc Natl Acad Sci USA. 107:2681–2686.

Flohr H, Glade U, Motzko D. 1998. The role of the NMDA synapse in general anesthesia. Toxicol Lett. 100–101:23–29.

Friston K. 2005. A theory of cortical responses. Philos Trans R Soc Lond, Ser B Biol Sci. 360:815–836.

Glover GH. 1999. Deconvolution of impulse response in event-related BOLD fMRI. NeuroImage. 9:416–429.

Goebel R, Esposito F, Formisano E. 2006. Analysis of functional image analysis contest (FIAC) data with brainvoyager QX: from single-subject to cortically aligned group general linear model analysis and self-organizing group independent component analysis. Hum Brain Mapp. 27:392–401.

Greve DN, Fischl B. 2009. Accurate and robust brain image alignment using boundary-based registration. NeuroImage. 48: 63–72.

Harrison SA, Tong F. 2009. Decoding reveals the contents of visual working memory in early visual areas. Nature. 458:632–635.

Herrero J, Gieselmann M, Sanayei M, Thiele A. 2013. Attention-induced variance and noise correlation reduction in macaque V1 is mediated by NMDA receptors. Neuron. 78:729–739.

Herrero J, Roberts M, Delicato L, Gieselmann M, Dayan P, Thiele A. 2008. Acetylcholine contributes through muscarinic receptors to attentional modulation in V1. Nature. 454:1110–1114.

Hochstein S, Ahissar M. 2002. View from the top: hierarchies and reverse hierarchies in the visual system. Neuron. 36:791–804.

Hsieh P-J, Vul E, Kanwisher N. 2010. Recognition alters the spatial pattern of FMRI activation in early retinotopic cortex. J Neurophysiol. 103:1501–1507.

Hubel DH, Wiesel TN. 1968. Receptive fields and functional architecture of monkey striate cortex. J Physiol. 195:215–243.

Imamoglu F, Kahnt T, Koch C, Haynes J-D. 2012. Changes in functional connectivity support conscious object recognition. NeuroImage. 63:1909–1917.

Kocsis B, Brown RE, McCarley RW, Hajos M. 2013. Impact of ketamine on neuronal network dynamics: translational modeling of schizophrenia-relevant deficits. CNS Neurosci Ther. 19: 437–447.

Koivisto M, Railo H, Revonsuo A, Vanni S, Salminen-Vaparanta N. 2011. Recurrent processing in V1/V2 contributes to categorization of natural scenes. J Neurosci. 31:2488–2492.

Kok P, Jehee JF, de Lange FP. 2012. Less is more: expectation sharpens representations in the primary visual cortex. Neuron. 75:265–270.

Kotermanski SE, Johnson JW, Thiels E. 2013. Comparison of behavioral effects of the NMDA receptor channel blockers memantine and ketamine in rats. Pharmacol Biochem Behav. 109:67–76.

Kriegeskorte N, Mur M, Ruff DA, Kiani R, Bodurka J, Esteky H, Tanaka K, Bandettini PA. 2008. Matching categorical object representations in inferior temporal cortex of man and monkey. Neuron. 60:1126–1141.

Lamme VAF, Zipser K, Spekreijse H. 1998. Figure-ground activity in primary visual cortex is suppressed by anesthesia. Proc Natl Acad Sci USA. 95:3263–3268.

Lamme VAF. 2006. Towards a true neural stance on consciousness. Trends Cogn Sci. 10:494–501.

Lee TS, Mumford D. 2003. Hierarchical Bayesian inference in the visual cortex. J Opt Soc Am. 20:1434–1448.

Lodge D, Johnson KM. 1990. Noncompetitive excitatory amino acid receptor antagonists. Trends Pharmacol Sci. 11:81–86.

Lumer ED, Edelman GM, Tononi G. 1997. Neural dynamics in a model of the thalamocortical system. I. Layers, loops and the emergence of fast synchronous rhythms. Cereb Cortex. 7:207–227.

Malach R, Reppas J, Benson R, Kwong K, Jiang H, Kennedy W, Ledden P, Brady T, Rosen B, Tootell R. 1995. Object-related activity revealed by functional magnetic resonance imaging in human occipital cortex. Proc Natl Acad Sci USA. 92: 8135–8139.

McKeeff TJ, Tong F. 2007. The timing of perceptual decisions for ambiguous face stimuli in the human ventral visual cortex. Cereb Cortex. 17:669–678.

Meuwese JDI, van Loon AM, Scholte HS, Lirk PB, Vulink NCC, Hollmann MW, Lamme VAF. 2013. NMDA receptor antagonist ketamine impairs feature integration in visual perception. PLoS ONE. 8:e79326.

Mooney CM. 1957. Age in the development of closure ability in children. Can J Psychol. 11:219.

Moore C, Cavanagh P. 1998. Recovery of 3D volume from 2-tone images of novel objects. Cognition. 67:45–71.

Newcomer JW, Krystal JH. 2001. NMDA receptor regulation of memory and behavior in humans. Hippocampus. 11:529–542.

Peelen MV, Fei-Fei L, Kastner S. 2009. Neural mechanisms of rapid natural scene categorization in human visual cortex. Nature. 460:94–97.

Poort J, Raudies F, Wannig A, Lamme VAF, Neumann H, Roelfsema PR. 2012. The role of attention in figure-ground segregation in areas V1 and V4 of the visual cortex. Neuron. 75:143–156.

Rao RP, Ballard DH. 1999. Predictive coding in the visual cortex: a functional interpretation of some extra-classical receptive-field effects. Nat Neurosci. 2:79–87.

Roelfsema PR, Lamme VAF, Spekreijse H, Bosch H. 2002. Figure-ground segregation in a recurrent network architecture. J Cognit Neurosci. 14:525–537.

Self MW, Kooijmans RN, Supèr H, Lamme VAF, Roelfsema PR. 2012. Different glutamate receptors convey feedforward and recurrent processing in macaque V1. Proc Natl Acad Sci USA. 109:11031–11036.

Smith SM, Jenkinson M, Woolrich MW, Beckmann CF, Behrens TE, Johansen-Berg H, Bannister PR, De Luca M, Drobnjak I, Flitney DE. 2004. Advances in functional and structural MR image analysis and implementation as FSL. NeuroImage. 23: S208–S219.

Summerfield C, Koechlin E. 2008. A neural representation of prior information during perceptual inference. Neuron. 59:336–347.

Taffe MA, Davis SA, Gutierrez T, Gold LH. 2002. Ketamine impairs multiple cognitive domains in rhesus monkeys. Drug Alcohol Depend. 68:175–187.

van Loon AM, Scholte HS, van Gaal S, van der Hoort BJJ, Lamme VAF. 2012. GABAA agonist reduces visual awareness: a masking-EEG experiment. J Cognit Neurosci. 24:965–974.

Vetter P, Grosbras M-H, Muckli L. 2013. TMS over V5 disrupts motion prediction. Cereb Cortex. doi: 10.1093/cercor/bht297.

Vetter P, Smith FW, Muckli L. 2014. Decoding sound and imagery content in early visual cortex. Curr Biol. 24:1256–1262.

Wokke ME, Sligte IG, Scholte HS, Lamme VAF. 2012. Two critical periods in early visual cortex during figure-ground segregation. Brain and Behav. 2:763–777.

Wokke ME, Vandenbroucke ARE, Scholte HS, Lamme VAF. 2013. Confuse your illusion: feedback to early visual cortex contributes to perceptual completion. Psychol Sci. 24:63–71.

Woolrich MW, Ripley BD, Brady M, Smith SM. 2001. Temporal autocorrelation in univariate linear modeling of FMRI data. NeuroImage. 14:1370–1386.

Wyatte D, Curran T, O'Reilly R. 2012. The limits of feedforward vision: Recurrent processing promotes robust object recognition when objects are degraded. J Cognit Neurosci. 24:2248–2261.

Yuille A, Kersten D. 2006. Vision as Bayesian inference: analysis by synthesis? Trends Cogn Sci. 10:301–308.